Instability of the Plane Poiseuille Flow for Longitudinal Vortical Disturbances by the Ghost Effect of Infinitesimal Curvature

Yoshio Sone* and Toshiyuki Doi†

*230-133 Iwakura-Nagatani-cho Sakyo-ku, Kyoto 606-0026, Japan
†Department Applied Mathematics and Physics, Tottori University, Tottori 680-8552, Japan

Abstract. The linear instability of the Poiseuille flow between two parallel plane walls of a gas in the continuum limit for longitudinal vortical disturbances is studied on the basis of the fluid-dynamic-type system derived as the continuum limit of the Boltzmann system in the process of which the behavior of the other parameters is taken into account. The amplifying factor and the frequency of the disturbances are obtained with the stability analysis. Owing to the ghost effect of infinitesimal curvature of the boundary, the Poiseuille flow can be unstable for longitudinal vortical disturbances.

INTRODUCTION

The authors recently proposed a new kind of ghost effect[1] in a gas in the continuum limit.[2, 3] That is, the behavior of parallel flows of a gas in the continuum limit between two parallel plane walls has been studied as the limit of nearly parallel flows between two rotating coaxial circular cylinders when the mean free path ℓ and the inverse of the radius L_A of the inner cylinder simultaneously tend to zero with the difference D of the radii of the two cylinders fixed, i.e., as $\ell/D \to 0$ and $D/L_A \to 0$. The fluid-dynamic-type equations and their boundary conditions describing the limiting behavior, derived by asymptotic analysis of the Boltzmann system, shows an interesting feature. They depend on the relative speed of decay of the two parameters, the Knudsen number $\mathrm{Kn} = \ell/D$ and the relative curvature D/L_A of the inner cylinder, and the infinitesimal curvature effect enters the fluid-dynamic-type equations if $(D/L_A)/\mathrm{Kn}^2$ remains at a finite value or diverges when $\mathrm{Kn} \to 0$.

In a channel between two parallel plane walls under the pressure gradient along the channel, it is known that a longitudinal vortical flow exists besides the well-known parallel flow with the parabolic profile (the plane Poiseuille flow).[4] However, the instability of the plane Poiseuille flow for longitudinal vortical disturbances is not known; thus, the relation of the two flows is unclear. In the present work, we study the stability of the Poiseuille flow for a longitudinal vortical disturbance on the basis of the system described in the last paragraph, and show that the flow can be unstable owing to the ghost effect of infinitesimal curvature. Thus, longitudinal vortical flows bifurcate from the Poiseuille flow.

BASIC EQUATION AND BOUNDARY CONDITION

Here, we consider a unidirectional parallel flow with a small but finite Mach number of a gas in the continuum limit between two parallel plane walls with small temperature difference[1] as the limit of a nearly parallel flow described in INTRODUCTION. The relative size $(D/L_A)/\mathrm{Kn}^2$ of the two parameters (D/L_A) and Kn^2 is taken here to be constant in the limit $\mathrm{Kn} \to 0$, because this is the threshold where the effect of infinitesimal curvature appears in the continuum limit. Let $D(x,y,z)$ be the Cartesian coordinate system with x being taken in the direction of the parallel flow and the two walls be at $y = 0$ and at $y = 1$. Let V be the characteristic speed of flow in the system. Then $V/(2RT_A)^{1/2}$, where T_A is the temperature of the wall at $y = 0$ and R is the specific gas constant, is a quantity of the order of the characteristic

[1] The temperature difference of the two plates divided by the temperature of one wall is a small quantity of the order of the Mach number.

Mach number and is put ε, which is small but finite. The quantity $(D/L_A)/\mathrm{Kn}^2$ that is kept constant in the limiting process is put $\pi/4(C\varepsilon)^2$, where C is a constant of the order of unity. Let the flow velocity be (v_x, v_y, v_z), which is assumed to be nearly parallel; that is, v_x is of the order of V or $\varepsilon(2RT_A)^{1/2}$, and v_y and v_z are infinitesimal quantities of the order of $\mathrm{Kn}(2RT_A)^{1/2}$. We put the flow velocity (v_x, v_y, v_z) and the pressure p of the gas in the form

$$\left.\begin{aligned} v_x &= \frac{VC\gamma_1}{2}\hat{u}_x, \quad (v_y, v_z) = \frac{(2RT_A)^{1/2}\gamma_1 k}{2}(\hat{u}_y, \hat{u}_z), \\ p &= p_0[1 + \varepsilon^2(\gamma_1 C)^2\hat{P}_{02}/2 + \cdots + k^2\gamma_1^2\hat{P}_{20}/2 + \cdots], \end{aligned}\right\} \tag{1}$$

where $(\hat{u}_x, \hat{u}_y, \hat{u}_z)$, $\hat{P}_{02}$, and $\hat{P}_{20}$ are quantities of the order of unity, $k = \sqrt{\pi}\mathrm{Kn}/2 = \sqrt{\pi}\ell/2D$ with ℓ being the mean free path of the gas in the equilibrium state at rest with temperature T_A and the average density ρ_0 of the gas in the domain, γ_1 is a constant that depends on the molecular model, e.g., $\gamma_1 = 1.270042$ (hard sphere gas) and $\gamma_1 = 1$ (BKW model), and the factors C and γ_1 are introduced to make the resulting equations independent of them. Then, the parallel flow field $\hat{u}_x$ varying slowly in space x and in the time scale of viscous diffusion is determined together with the amplified infinitesimal cross flow field $(\hat{u}_y, \hat{u}_z)$, independently of the temperature field by the following fluid-dynamic-type equations and their associated boundary conditions: the equations are

$$\frac{\partial \hat{P}_{02}}{\partial y} = \frac{\partial \hat{P}_{02}}{\partial z} = 0, \tag{2}$$

$$\frac{\partial \hat{u}_x}{\partial \bar{\chi}} + \frac{\partial \hat{u}_y}{\partial y} + \frac{\partial \hat{u}_z}{\partial z} = 0, \tag{3a}$$

$$\frac{\partial \hat{u}_x}{\partial \tilde{t}} + \hat{u}_x\frac{\partial \hat{u}_x}{\partial \bar{\chi}} + \hat{u}_y\frac{\partial \hat{u}_x}{\partial y} + \hat{u}_z\frac{\partial \hat{u}_x}{\partial z} = -\frac{\partial \hat{P}_{02}}{\partial \bar{\chi}} + \frac{\partial^2 \hat{u}_x}{\partial y^2} + \frac{\partial^2 \hat{u}_x}{\partial z^2}, \tag{3b}$$

$$\frac{\partial \hat{u}_y}{\partial \tilde{t}} + \hat{u}_x\frac{\partial \hat{u}_y}{\partial \bar{\chi}} + \hat{u}_y\frac{\partial \hat{u}_y}{\partial y} + \hat{u}_z\frac{\partial \hat{u}_y}{\partial z} - \hat{u}_x^2 = -\frac{\partial \hat{P}_{20}}{\partial y} + \frac{\partial^2 \hat{u}_y}{\partial y^2} + \frac{\partial^2 \hat{u}_y}{\partial z^2}, \tag{3c}$$

$$\frac{\partial \hat{u}_z}{\partial \tilde{t}} + \hat{u}_x\frac{\partial \hat{u}_z}{\partial \bar{\chi}} + \hat{u}_y\frac{\partial \hat{u}_z}{\partial y} + \hat{u}_z\frac{\partial \hat{u}_z}{\partial z} = -\frac{\partial \hat{P}_{20}}{\partial z} + \frac{\partial^2 \hat{u}_z}{\partial y^2} + \frac{\partial^2 \hat{u}_z}{\partial z^2}, \tag{3d}$$

where $\bar{\chi}$ is the shrunk variable of x and $\tilde{t}$ is the shrunk variable of the time t, i.e.,

$$\bar{\chi} = kx/C\varepsilon, \quad \tilde{t} = t/[2D/\gamma_1(2RT_A)^{1/2}k], \tag{4}$$

where $D/\gamma_1(2RT_A)^{1/2}k$ is the time scale of viscous diffusion, and the boundary conditions[2] are

$$\hat{u}_x = \hat{u}_A, \ \hat{u}_y = \hat{u}_z = 0 \quad \text{at } y = 0, \tag{5a}$$

$$\hat{u}_x = \hat{u}_B, \ \hat{u}_y = \hat{u}_z = 0 \quad \text{at } y = 1, \tag{5b}$$

where $\hat{u}_A$ and $\hat{u}_B$ are given by the velocities v_A and v_B of the walls moving in their plane as

$$\hat{u}_A = v_A/(VC\gamma_1/2), \quad \hat{u}_B = v_B/(VC\gamma_1/2). \tag{6}$$

STABILITY OF POISEUILLE FLOW

Analysis

The system (2)–(3d), (5a), and (5b) has the following simple solution when $\hat{u}_B = \hat{u}_A$:

$$\left.\begin{aligned} &\hat{u}_x = U_U = \hat{u}_A + 12y(1-y)/\gamma_1 C, \quad \hat{u}_y = \hat{u}_z = 0, \\ &\hat{P}_{02} = \hat{P}_{02U} = -24\bar{\chi}/\gamma_1 C, \\ &\hat{P}_{20} = \hat{P}_{20U} = \hat{u}_A^2 y + 4\hat{u}_A y^2(3-2y)/\gamma_1 C + 144y^3(\tfrac{1}{3} - \tfrac{1}{2}y + \tfrac{1}{5}y^2)/(\gamma_1 C)^2 + g(\bar{\chi}), \end{aligned}\right\} \tag{7}$$

[2] Infinitesimal speeds of the walls affect the flow field. Here, we consider the case in which they are higher-order infinitesimal.

where $g(\bar{\chi})$ is a function of $\bar{\chi}$ to be determined in the higher-order analysis.[3] This is the well-known plane Poiseuille flow. The volume flow rate of the flow through the channel in the unit width is given by VD, and the pressure gradient $\partial p/\partial Dx$ by $-12\gamma_1 k[V/(2RT_A)^{1/2}](p_0/D)$, which is infinitesimal of the order of k.[4]

We will consider the linear instability of the Poiseuille flow (7) for the longitudinal vortical disturbance. First, the solution of the system (2)–(3d), (5a), and (5b) is put in the form of the perturbation of the Poiseuille flow (7), i.e.,

$$\hat{u}_x = U_U + U_1,\ \hat{u}_y = V_1,\ \hat{u}_z = W_1,\ \hat{P}_{02} = \hat{P}_{02U} + \mathscr{P}_{02},\quad \hat{P}_{20} = \hat{P}_{20U} + \mathscr{P}_{20}. \tag{8}$$

Substituting Eq. (8) into Eqs. (2)–(3d), (5a), and (5b), and neglecting the second-order terms of the perturbation and the higher, we obtain the linear partial differential equations for $(U_1, V_1, W_1, \mathscr{P}_{02}, \mathscr{P}_{20})$

$$\frac{\partial \mathscr{P}_{02}}{\partial y} = \frac{\partial \mathscr{P}_{02}}{\partial z} = 0, \tag{9}$$

$$\frac{\partial U_1}{\partial \bar{\chi}} + \frac{\partial V_1}{\partial y} + \frac{\partial W_1}{\partial z} = 0, \tag{10a}$$

$$\frac{\partial U_1}{\partial \tilde{t}} + U_U \frac{\partial U_1}{\partial \bar{\chi}} + \frac{\mathrm{d}U_U}{\mathrm{d}y} V_1 = -\frac{\partial \mathscr{P}_{02}}{\partial \bar{\chi}} + \frac{\partial^2 U_1}{\partial y^2} + \frac{\partial^2 U_1}{\partial z^2}, \tag{10b}$$

$$\frac{\partial V_1}{\partial \tilde{t}} + U_U \frac{\partial V_1}{\partial \bar{\chi}} - 2U_U U_1 = -\frac{\partial \mathscr{P}_{20}}{\partial y} + \frac{\partial^2 V_1}{\partial y^2} + \frac{\partial^2 V_1}{\partial z^2}, \tag{10c}$$

$$\frac{\partial W_1}{\partial \tilde{t}} + U_U \frac{\partial W_1}{\partial \bar{\chi}} = -\frac{\partial \mathscr{P}_{20}}{\partial z} + \frac{\partial^2 W_1}{\partial y^2} + \frac{\partial^2 W_1}{\partial z^2}, \tag{10d}$$

and the boundary conditions

$$U_1 = V_1 = W_1 = 0 \ \text{ at } y = 0 \text{ and } y = 1. \tag{11}$$

Here, we consider the perturbation in the form of a longitudinal vortical flow. That is, we look for the solution of the above linear system with the real coefficients in the form

$$(U_1, V_1, W_1, \mathscr{P}_{02}, \mathscr{P}_{20}) = \mathrm{Rp}([\mathbf{U}, \mathbf{V}, \mathbf{W}, 0, \mathbf{P}] \exp[\lambda \tilde{t} - \mathrm{i}(\beta \bar{\chi} + \alpha z)]), \tag{12}$$

where i is the imaginary unit, α and β are real constants, λ is a complex constant, $\mathbf{U}$, $\mathbf{V}$, $\mathbf{W}$, and $\mathbf{P}$ are complex-valued functions of y, Rp indicates the real part, and the relation $\mathscr{P}_{02} = 0$ is due to the consistency with Eq. (9). Then, substituting Eq. (12) into Eqs. (10a)–(11), we obtain the linear ordinary differential equations for $(\mathbf{U}, \mathbf{V}, \mathbf{W}, \mathbf{P})$

$$\left.\begin{aligned} &-\mathrm{i}\beta\mathbf{U} + \frac{\mathrm{d}\mathbf{V}}{\mathrm{d}y} - \mathrm{i}\alpha\mathbf{W} = 0, \quad \frac{\mathrm{d}^2\mathbf{U}}{\mathrm{d}y^2} - (\alpha^2 + \lambda - \mathrm{i}\beta U_U)\mathbf{U} - \frac{\mathrm{d}U_U}{\mathrm{d}y}\mathbf{V} = 0, \\ &\mathrm{i}\alpha\left[2U_U\mathbf{U} + \frac{\mathrm{d}^2\mathbf{V}}{\mathrm{d}y^2} - (\alpha^2 + \lambda - \mathrm{i}\beta U_U)\mathbf{V}\right] + \frac{\mathrm{d}^3\mathbf{W}}{\mathrm{d}y^3} - (\alpha^2 + \lambda - \mathrm{i}\beta U_U)\frac{\mathrm{d}\mathbf{W}}{\mathrm{d}y} + \mathrm{i}\beta\frac{\mathrm{d}U_U}{\mathrm{d}y}\mathbf{W} = 0, \end{aligned}\right\} \tag{13}$$

$$\mathbf{P} = \frac{\mathrm{i}}{\alpha}\left[\frac{\mathrm{d}^2\mathbf{W}}{\mathrm{d}y^2} - (\alpha^2 + \lambda - \mathrm{i}\beta U_U)\mathbf{W}\right], \tag{14}$$

and the boundary condition

$$\mathbf{U}(y) = \mathbf{V}(y) = \mathbf{W}(y) = 0 \ \text{ at } y = 0 \text{ and } y = 1. \tag{15}$$

The system, containing the parameters α, β, λ, $1/\gamma_1 C$, and $\hat{u}_A$, is linear and homogeneous. For the system to have a solution, these parameters must satisfy some relations, i.e.,

$$\lambda_r = \lambda_r(\alpha, \beta, 1/\gamma_1 C, \hat{u}_A),\ \ \lambda_i = \lambda_i(\alpha, \beta, 1/\gamma_1 C, \hat{u}_A), \tag{16}$$

---

[3] This function does not contribute to the following stability analysis.

[4] (i) In the dimensional variables, the velocity and pressure are independent of C (or the relative limiting speed) except for the infinitesimal of the order of k^2 and the higher.

(ii) In this simple solution, the motion of the wall is unimportant, because it is just a translation.

where λ_r and λ_i are, respectively, the real and imaginary parts of λ. The plane Poiseuille flow is linearly unstable for a longitudinal vortical disturbance when $\lambda_r > 0$, and it is stable when $\lambda_r < 0$. Here, it may be better to note the interpretation of the result, because the characteristic speed V of the Poiseuille flow does not apparently enter the result. We are considering the limiting case in which the Knudsen number Kn and the relative curvature D/L_A vanish keeping $(D/L_A)/\mathrm{Kn}^2$ fixed (say, at $\hat{c}_0^{-2}$). Here we have chosen $V/(2RT_A)^{1/2}$, where V is the average flow speed of the Poiseuille flow, as ε. Thus, $CV/(2RT_A)^{1/2} = \sqrt{\pi}\hat{c}_0/2$. That is, $1/\gamma_1 C$ is expressed with V and c_0 as[5]

$$1/\gamma_1 C = (2/\sqrt{\pi})[V/(2RT_A)^{1/2}]/\hat{c}_0\gamma_1. \tag{17}$$

The expression (12) for the perturbation $(U_1, V_1, W_1, \mathscr{P}_{20})$ can be transformed in the form

$$U_1 = (\bar{\mathbf{U}}\mathbf{U})^{1/2}\exp(\lambda_r\tilde{t})\cos(\beta\bar{\chi} + \alpha z - \lambda_i\tilde{t} - \varphi_U), \quad \mathbf{U} = (\bar{\mathbf{U}}\mathbf{U})^{1/2}\exp(\mathrm{i}\varphi_U), \tag{18}$$

and U_1, $\mathbf{U}$, and φ_U are replaced by the corresponding functions for the functions V_1, W_1, and $\mathscr{P}_{20}$. The translation given by $\varphi_U + \varphi_0$, $\varphi_V + \varphi_0$, $\varphi_W + \varphi_0$, and $\varphi_{\mathscr{P}} + \varphi_0$, where φ_0 is an arbitrary constant, is also the solution. In view that $\bar{\chi}$ is the infinitesimally shrunk variable defined by Eq. (4), the perturbation is a travelling wave, uniform in x, periodic in z, and is propagating in the $\pm z$ direction, with $z =$ const being infinitesimally deflected to $\beta kx/C\varepsilon + \alpha z =$ const. Let $(\mathbf{U}, \mathbf{V}, \mathbf{W}, \lambda)$ be the solution for $(\alpha, \underline{\beta}, \underline{1/\gamma_1 C}, \hat{u}_A)$. Then, obviously from Eqs. (13)–(15), $(\mathbf{U}, \mathbf{V}, -\mathbf{W}, \lambda)$ is a solution for $(-\alpha, \beta, 1/\gamma_1 C, \hat{u}_A)$, and $(\bar{\mathbf{U}}, \bar{\mathbf{V}}, -\bar{\mathbf{W}}, \lambda)$ is a solution for $(\alpha, -\beta, 1/\gamma_1 C, \hat{u}_A)$, and vice versa, where the bar – over the complex variables $(\mathbf{U}, \mathbf{V}, \mathbf{W}, \lambda)$ indicates their complex conjugates. Thus, it is enough to consider the case for $\alpha \geq 0$ and $\beta \geq 0$. The latter two solutions are the same solution and the mirror image with respect to $z = 0$ of that for $(\alpha, \beta, 1/\gamma_1 C, \hat{u}_A)$. The proof in APPENDIX in [5] applies to the present case as it is, because the explicit form of U_U is not used there. Thus, $\lambda_i = 0$ or the solution is not oscillating when $\beta = 0$.

Numerical Results

We will summarized the result, especially the relation (16), of the homogeneous boundary-value problem (13)–(15) obtained by numerical computation, which can be done in a procedure similar to that of bifurcation analysis in Bénard problem in [5] or [3]. First, take the case when both the walls are at rest, i.e., $\hat{u}_A = \hat{u}_B = 0$. Figure 1 (a) shows the neutral surface $\lambda_r = 0$ in the space $(\alpha, \beta, 1/\gamma_1 C)$ and the corresponding values of λ_i on it, that is, level lines $1/\gamma_1 C =$ const and $\lambda_i =$ const for $\lambda_r = 0$ are drawn in the plane $(\alpha/\pi, \beta/\pi)$. Figure 1 (b) shows level lines $\lambda_r =$ const and $\lambda_i =$ const in the plane $(\beta/\pi, 1/\gamma_1 C)$ when $\alpha/\pi = 1$. Generally, the homogeneous boundary-value problem (13)–(15) has infinitely many solutions, thus infinite sets of (λ_r, λ_i), for a given set of the parameters α, β, and $1/\gamma_1 C$. Thus in panel (a), the neutral surface with the smallest $1/\gamma_1 C$ is shown, because λ_r is shown numerically to be negative for $1/\gamma_1 C$ smaller than this value. The neutral surface folds back along the dot-dash line, across which no neutral surface exists or min $1/\gamma_1 C$ is discontinuous, and the surface going to higher $1/\gamma_1 C$ folds back again and extends further from the dot-dash line (see the right upper corner of the figure). The computation is carried out up to $1/\gamma_1 C = 2500$ below which the neutral surface does not appear in the right lower half of the domain. It may be noted that λ_r is positive just above this neutral surface but that λ_r can be negative above the neutral surface between other neutral surfaces. In panel (b), the largest values of λ_r and the values of λ_i of the corresponding solution are shown; a family of solutions that vary with the parameters does not always take the largest λ_r in the plane $(\beta/\pi, 1/\gamma_1 C)$, but another family takes the largest λ_r is some part of the plane; the intersection of the two regions is shown in a dot-dash line in the panel (b); naturally, the level lines $\lambda_i =$ const are generally discontinuous there.

Next, the effect of $\hat{u}_A$ on (λ_r, λ_i) is studied. Figure 2 shows the level lines $\lambda_r =$ const and $\lambda_i =$ const in the plane $(\hat{u}_A, 1/\gamma_1 C)$. As in Fig. 1, we are interested in the solution with the largest value of λ_r for a given set of $(\hat{u}_A, 1/\gamma_1 C)$. Panel (a) is for the case $(\alpha = \pi, \beta = 0)$, for which λ_i is always zero as already explained, and panel (b) is for the case $(\alpha = \pi, \beta = \pi)$. There is a neutral line in the region $\hat{u}_A < 0$ that does not pass $\hat{u}_A = 0$. There is a region where the solution is stable $(\lambda_r < 0)$ in the central part between the two neutral curves $(\lambda_r = 0)$. In addition to the situation of the surface max $\lambda_r(\hat{u}_A, 1/\gamma_1 C)$ mentioned in the explanation of Fig. 1 (b), the surface λ_r formed by a family of solutions can be multi-valued. Thus, the surface max λ_r is discontinuous [panel (a)] or is not smooth [panel (b)]. These points

[5] If you choose a different quantity as ε, the formula is apparently different, but the content is the same. One has to leave the freedom in the relation between the characteristic speed V and $\hat{c}_0$. If you choose VC as new V, then you loose the freedom in choosing the two parameters, characteristic flow speed and the ratio of the curvature to the Knudsen number squared.

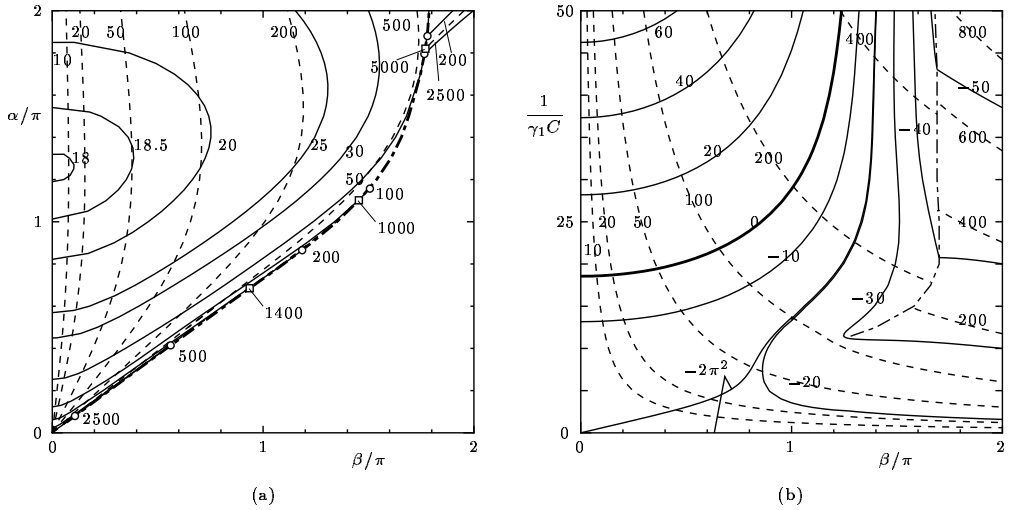

FIGURE 1. Stability diagram I: the two walls are at rest ($v_A = v_B = 0$). (a) Neutral surface in the space $(\alpha/\pi, \beta/\pi, 1/\gamma_1 C)$ and λ_i on the surface, and (b) level lines $\lambda_r = \text{const}$ (solid lines) and $\lambda_i = \text{const}$ (dashed line) in the plane $(\beta/\pi, 1/\gamma_1 C)$ when $\alpha/\pi = 1$. In panel (a), level lines $1/\gamma_1 C = \text{const}$ (solid lines —) and $\lambda_i = \text{const}$ (dashed lines - - -) for $\lambda_r = 0$ are drawn in the plane $(\alpha/\pi, \beta/\pi)$. Generally, there are infinite number of solutions, thus infinite sets of (λ_r, λ_i) for a given set of the parameters α, β, and $1/\gamma_1 C$. Thus in panel (a), the neutral surface with the smallest $1/\gamma_1 C$ is shown. The neutral surface folds back along the dot-dash line, across which no neutral surface exists or min $1/\gamma_1 C$ is discontinuous, and the surface going to higher $1/\gamma_1 C$ folds back and extends further from the dot-dash line (see the right upper corner of the figure). The numerical data at the circles ∘ and at the squares □ on the dot-dash line are, respectively, the values of $1/\gamma_1 C$ and λ_i there. The computation is carried out up to $1/\gamma_1 C = 2500$ below which the neutral surface does not appear in the right lower half of the domain. In panel (b), the largest values of λ_r and the values of λ_i of the corresponding solution are shown; a family of solutions does not always take the largest λ_r in the plane $(\beta/\pi, 1/\gamma_1 C)$, but another family of solutions takes the largest λ_r in some part of the plane; the intersection of the two regions is shown in a dot-dash line in the panel (b); naturally, the level lines $\lambda_i = \text{const}$ are generally discontinuous there. Note $2\pi^2 = 19.7392\cdots$.

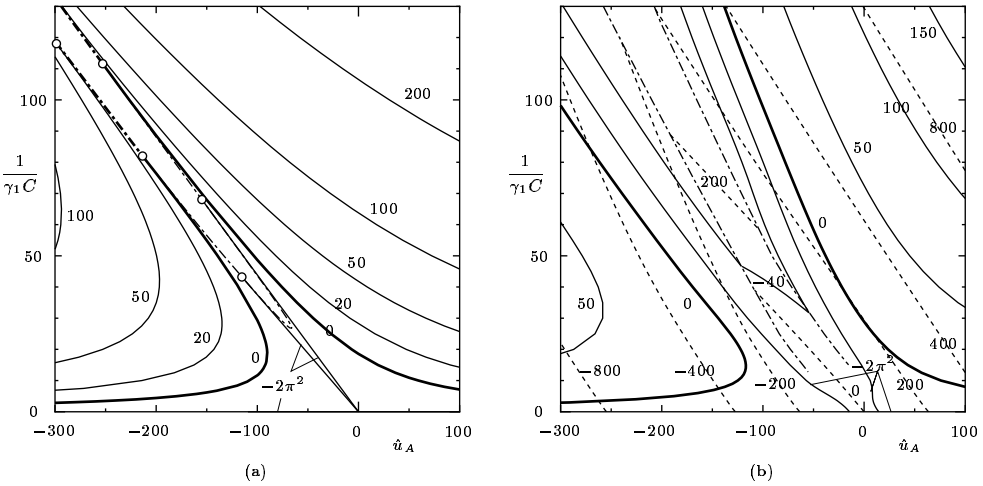

FIGURE 2. Stability diagram II: The level lines $\lambda_r = \text{const}$ and $\lambda_i = \text{const}$ in the plane $(\hat{u}_A, 1/\gamma_1 C)$, when two walls are moving with the same velocity. (a) $\alpha = \pi, \beta = 0$, and (b) $\alpha = \pi, \beta = \pi$. The solid lines — are $\lambda_r = \text{const}$, and the dashed lines - - - are $\lambda_i = \text{const}$. The largest values of λ_r and the values of λ_i of the corresponding solution are shown. The max λ_r [panel (a)] and its derivative [panel (b)] across the dot-dash lines – - – are discontinuous; the λ_i is discontinuous there. The circles ∘ on the dot-dash line in panel (a) show that the corresponding level lines $\lambda_r = \text{const}$ cease to be max λ_r there, because the surface λ_r of a family of solutions folds back there; in the narrow region surrounded by the dot-dash line, λ_r is negative. The discontinuity of max λ_r exists in this negative λ_r region but is not shown here.

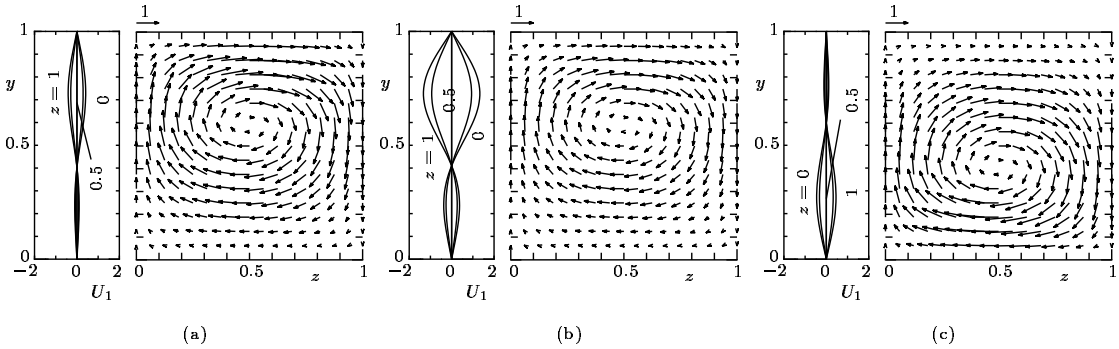

FIGURE 3. Eigenfunctions (U_1, V_1, W_1) of the perturbation on the neutral line ($\alpha = \pi$ and $\beta = 0$). (a) $(\hat{u}_A, 1/\gamma_1 C) = (200, 3.9873)$, (b) $(\hat{u}_A, 1/\gamma_1 C) = (0, 18.5675)$, and (c) $(\hat{u}_A, 1/\gamma_1 C) = (-200, 4.4172)$. In each panel, the profile of U_1 at $z = 0$, 0.25, 0.5, 0.75, and 1 and the cross field (V_1, W_1) are shown. The arrows are (V_1, W_1) at their starting points and their scale 1 is shown on the left shoulder of each figure.

are shown by dot-dash lines. The λ_i is generally discontinuous across these lines. The behavior of the level lines $\lambda_r =$ const and $\lambda_i =$ const are delicate in narrow regions near the edges of the dot-dash lines in the stable region ($\lambda_r < 0$), which is not shown here. Obviously, from these figures, the flow is more unstable when $\hat{u}_A \neq 0$.

The result of the present analysis apparently is not Galilean invariant, i.e., uniform parallel motion of the walls modifies the stability. However, careful examination is required for correct understanding. The solution of the problem is not unique; it depends on the limiting process. The correct correspondence of the limiting processes in two inertial systems corresponding to a given physical situation gives the solutions related by the Galilean transformation. If the common axis of the cylinders is at rest in one system, the axis is moving in the other system; thus, the solution with the wall velocities in boundary conditions (5a) and (5b) being shifted is not an appropriate correspondence in the moving system. The above apparent violence of Galilean invariance is due to the inappropriate correspondence. More explanation is found in [3].

Eigenfunctions (U_1, V_1, W_1) of the disturbance for $\alpha = \pi$ and $\beta = 0$ are shown for three different $\hat{u}_A$'s in Fig. 3, where it is made definite by $\int_0^1 (\mathbf{U}\overline{\mathbf{U}} + \mathbf{V}\overline{\mathbf{V}} + \mathbf{W}\overline{\mathbf{W}})\mathrm{d}y = 1$. It may be noted that owing to the relation (1), the cross flow (v_y, v_z) is infinitesimal, but the disturbance to the main flow corresponding to U_1 is finite.

CONCLUDING REMARKS

We have studied the linear stability of the plane Poiseuille flow for longitudinal vortical disturbances on the basis of the system derived from the Boltzmann system in the continuum limit where the curvature of the boundary wall vanishes together with the Knudsen number. Owing to the ghost effect of infinitesimal curvature, the flow can be unstable. That is, owing to the infinitesimal curvature of the boundary, infinitesimal cross flow field is amplified, and the main flow becomes unstable by the convection effect of the cross flow. The present choice of parameters, i.e., the Mach number is finite and the Knudsen number is infinitesimal, corresponds to infinite Reynolds number. Thus, the longitudinal vortical disturbances bifurcate at infinite Reynolds number. In the atmospheric condition, the mean free path is very small but finite; thus, the instability takes place only when the curvature of the boundary is finite. However, in a flow in a channel with $D = 10$ cm and $V = 50$ cm/s, the instability due to the curvature effect appears when the curvature is larger than $1/1000\ \mathrm{m}^{-1}$. In other words, we have to control this size of curvature to eliminate its effect.

REFERENCES

1. Y. Sone, *Kinetic Theory and Fluid Dynamics*, Birkhäuser, Boston, 2002.
2. Y. Sone and T. Doi, *Phys. Fluids* **16**, 952–971 (2004).
3. Y. Sone, *Molecular Gas Dynamics*, Birkhäuser, Boston, 2006.
4. F. Waleffe, *Phys. Fluids* **15**, 1517–1534 (2003).
5. Y. Sone and T. Doi, *Rarefied Gas Dynamics*, AIP, Melville, NY, 258–263 (2005).